Demixing Transition of the Aqueous Solution of Amyloidogenic Peptides: A REMD Simulation Study

ARTICLE *in* THE JOURNAL OF PHYSICAL CHEMISTRY B · AUGUST 2009

Impact Factor: 3.3 · DOI: 10.1021/jp901144v · Source: PubMed

4 AUTHORS, INCLUDING:

Ivan V. Brovchenko
Technische Universität Dortmund
92 PUBLICATIONS **1,648** CITATIONS
SEE PROFILE

Alla Oleinikova
Technische Universität Dortmund
91 PUBLICATIONS **2,667** CITATIONS
SEE PROFILE

Demixing Transition of the Aqueous Solution of Amyloidogenic Peptides: A REMD Simulation Study

Gurpreet Singh, Ivan Brovchenko, Alla Oleinikova,* and Roland Winter

Physical Chemistry, TU Dortmund University, Otto-Hahn-Str. 6, Dortmund, D-44227, Germany

Received: February 7, 2009; Revised Manuscript Received: May 5, 2009

The aggregation of amyloidogenic peptides in liquid water is studied at various temperatures by replica exchange molecular dynamics (REMD) simulations. The formation of a peptide aggregate upon decreasing the temperature reveals features typical for a first-order demixing phase transition, which is smeared out due to the finite size of the simulation box. Various properties of the ensemble of peptides were used to describe the temperature-induced demixing phase transition, which was found to occur at about 375 K. The hydrational and volumetric properties of the peptides and their aggregates are analyzed.

Introduction

Aggregation of biomolecules in an aqueous environment is a common phenomenon involved in various biologically important processes and diseases. An important example is the process of amyloid fibril formation, which is a key event in diverse pathological conditions such as Alzheimer's disease and type II diabetes mellitus. Experimental studies have demonstrated that the aggregation process shows features typical for a nucleation process in a system undergoing a first-order phase transition. In particular, aggregation occurs when the concentration of the biomolecules in the solution exceeds a certain critical value, which in turn depends on various parameters, such as the chemical structure of the biomolecule, temperature, ionic strength, pH, etc.[1−5] The lag time of aggregation decreases with increasing concentration beyond the critical concentration. It is reasonable to relate the aggregation behavior of biomolecules in liquid water to the demixing phase transition, which is a common phenomenon for aqueous solutions of organic molecules.[6] Upon demixing, the solution separates into a water-rich phase and an organic-rich phase. Often, the two coexisting phases are liquids, as both pure water and pure organic fluid are in the liquid state at the temperatures and pressures studied. In the case of macromolecules, such as polymers and proteins, the phase state of the pure solute is often solidlike (either amorphous or crystalline). Therefore, the organic-rich phase emerging upon demixing can also be solidlike and can precipitate from the solution. The demixing transition of the aqueous solutions of organic molecules, polymers, or biomolecules can occur both upon cooling and upon heating. For example, the heat-induced denaturation of proteins is often accompanied by their aggregation into an organic-rich phase.

Despite the common nature of the demixing transition in various aqueous solutions, aggregation of amyloidogenic peptides in water is often considered as a particular phenomenon, thus neglecting the general features common for all phase transitions. One of the important peculiarities of amyloidogenic peptides is their extremely low solubility in liquid water. The critical concentration, or solubility limit, at biologically relevant thermodynamic conditions is generally below the nanomolar range.[4] Above the critical concentration, the equilibrated aqueous solutions of such biomolecules consist of a water-rich phase with the critical peptide concentration and an organic-rich phase with a low amount of water. However, due to the low critical concentration, the formation of the equilibrated phases may take extremely long times.[3] Another peculiarity of the demixing transition in aqueous solutions of amyloidogenic peptides and proteins is a specific structure of the organic-rich phase which appears as a fibrillar aggregate with ordered arrangement of the biomolecules. These peculiarities of the demixing phenomenon in aqueous solution of amyloidogenic peptides have impact on the studies of aggregation in silico as well (see, for example, refs 7−10). Such studies are mainly focused on the kinetics and degree of peptide aggregation in oversaturated solutions, as well as on the structure of the aggregates in dependence of the chemical structure of the peptides. However, the demixing transition itself, which occurs upon varying temperature and/or pressure, attracted much less attention. In particular, the effect of temperature on peptide aggregation was addressed in a few papers only.[11−13] Moreover, to the best of our knowledge, a temperature-induced demixing phase transition between aggregated and disaggregated states of a peptide system has not been addressed using *explicit* water models.

The recent simulation studies of the demixing transitions in oversaturated peptide solutions indicate that the general properties of the first-order phase transition are clearly manifested in such systems. The dissolution of a protein aggregate in small systems is one of the examples.[6] This phenomenon originates from the effect of the finite system size on the stability of the minor phase in an oversaturated system. In a macroscopic (infinitely large) system, an equilibrium state appears as a coexistence of two stable phases, whereas in a small (finite) system, a new stable state with a dissolved minor phase appears.[14] In aqueous solutions of biomolecules, this phenomenon causes a distortion or even breakup of the biomolecular aggregate in a small system, whereas this aggregate is stable in the corresponding macroscopic system. This effect may be responsible for the difference in peptide aggregation inside and outside the small biological cells and their compartments in vivo. Besides, such an effect should be taken into account wherever aggregation is studied in silico using relatively small simulation boxes (see ref 6 for more details).

In the present paper, we study the temperature-induced demixing transition of the aqueous solution of amyloidogenic

* To whom correspondence should be addressed. E-mail: alla@pc2a.chemie.uni-dortmund.de.

10.1021/jp901144v CCC: $40.75
Published on Web 07/01/2009

peptides in explicit water by molecular dynamics simulations. We show that the peptides form an aggregate coexisting with a water-rich phase at low temperatures, whereas a soluble (one-phase) solution of peptides appears upon increasing temperature and pressure. Various parameters of the peptide system were tested with respect to their ability to describe the temperature-induced demixing transition and to estimate the temperature of the transition. A suitable order parameter of the phase transition, which vanishes in the one-phase region, is proposed. Common features of the demixing transitions in the water−peptide system and aqueous solutions of simpler organic molecules are discussed. The effects of temperature and pressure on the properties of the peptides and the hydration water are also analyzed. The pentapeptide fragment of the human islet amyloid polypeptide (hIAPP), corresponding to the amino acid residue 15−19, was chosen as a model peptide. It is one of the shortest peptide fragments of hIAPP capable of fibrillar self-assembly. Experimental studies have reported that the aqueous solution of the fragment forms broad ribbonlike fibrils.[15] The lag time is also expected to be very short, hence making it an ideal candidate for protein aggregation studies using molecular simulations.

Methods

Meaningful simulation studies of complex biomolecular systems, such as aqueous solutions of peptides, need the sampling of a huge configurational space and therefore are extremely time-consuming. This problem can partially be overcome by the parallel tempering technique (or replica exchange algorithm),[16,17] which provides an enhanced sampling of the configurational space of a system. This method was applied to simulation of biomolecules in 1997[18] and has thereafter been extended to molecular dynamics simulations.[19] Replica exchange molecular dynamics (REMD) simulations were applied also to study the effect of temperature on peptide aggregation in water.[11−13]

In constant volume REMD simulations, multiple copies (or replicas) of identical systems are simulated in parallel at different temperatures and pressures. The state-exchange moves are attempted periodically during which two neighboring replicas exchange their thermodynamic state (their temperatures). Such random walk in the temperature space allows individual replicas to sample a range of temperatures. At higher temperatures, the increased thermal energy facilitates the exploration of configurational space and allows the system to cross barriers, which cannot be crossed at the temperature of interest on the time scale of the simulation run. In case of solutions of biomolecules, REMD simulations sometimes allow a notable improvement of the conformational sampling, especially, at low temperatures.[20,21]

At regular intervals, pairs of replicas are exchanged according to a Metropolis criterion.[19] The acceptance probability P_{acc} for each state-exchange move between two neighboring states i and j is chosen to be

$$P_{acc} = \min\{1, \exp[(1/k_B T_i - 1/k_B T_j)(U(r_i^N) - U(r_j^N))]\} \quad (1)$$

where $U(r_i^N)$ is the configurational energy of the system in state i. This preserves the detailed balance, which is a sufficient condition for sampling from the Boltzmann distribution. The exchange of thermodynamic states between two replicas is justified for one-phase states only. Therefore, if the studied thermodynamic range includes a phase transition, simulations can be distorted by the exchange between one-phase and two-phase states. This distortion presumably appears as a smearing out of the first-order phase transition and can affect various system properties. However, in small systems, this effect can be neglected in comparison with the enormous effect of the finite system size on the phase transition.[6]

The simulated system consists of 12 peptide fragments having the amino acid sequence FLVHS (residues 15−19 of the hIAPP) and 3079 water molecules, corresponding to a peptide concentration of $C = 12.4$ wt %. The N- and C-termini of the peptide fragments were capped with acetyl and methylamide groups, respectively. A modified AMBER force field[22] was used for the peptides and the TIP3P model[23] for water. REMD simulations were performed in the constant volume ensemble,[19] using the RPMDRUN package.[24] Temperature spacing was calculated by performing initial uncoupled simulations for 0.5 ns at 36 different temperatures spanning from 275 to 991 K. The average energies were fitted with a polynomial and eq 1 was solved iteratively for a temperature distribution such that $P_{acc} = 0.20$. Sixty replicas, distributed over a temperature range from 286.7 to 645.5 K were used with a state exchange probability of 0.1, leading to a time interval of about 3 ps between two state exchanges for each replica. SHAKE was applied to constrain all bonds allowing the integration time step of 2.0 fs.[25] Electrostatic interactions were treated by particle mesh Ewald summation.[26] Simulations with 60 replicas were performed for 49 ns, corresponding to the total simulation time of 2.94 μs.

The degree of peptide aggregation was analyzed using the total radius of gyration R_g of all peptides as well as the properties of peptide clusters. Calculation of the radius of gyration R_g of a system of particles requires the knowledge of the center of mass of the system. In the simulation box with periodic boundary conditions, the position of the center of mass is not unique, as different choices of the origin of coordinates yield different positions of the center of mass, and, accordingly, different values of R_g. In the present study, R_g of all peptides was calculated by iteratively placing the origin of coordinates on the center of mass of each peptide. The minimum value of R_g obtained in this way was used as a measure of the compactness of the peptide system.

An analysis of peptide clustering is based on some criteria for the connectivity between two peptides. All the peptides linked via an intact chain of connected peptides are considered as members of the same cluster. Two different connectivity criteria were used in our studies. According to the first criterion, two peptides were considered as being connected if the distance between their centers of mass was less than or equal to 1.1 nm.[6] The connectivity criterion of 1.1 nm originates from the structure of fibrillar aggregates and corresponds to the intersheet distance.[27] The second criterion was based on the number of hydrophobic contacts between two peptides and the clusters calculated based on this connectivity criterion will be further called "hydrophobic clusters". A hydrophobic contact was considered to be present if the distance between two carbon atoms of nonpolar side chains F, L, and V of two peptides did not exceed the sum of the atomic van der Waals radii plus 0.28 nm, corresponding to the effective size of water molecule. Such definition ensures absence of a water molecule between hydrophobic side chains. Two peptides were considered to be connected if they have at least 10 hydrophobic contacts between them. The dependence of the aggregation parameters on the connectivity criteria has been analyzed in detail in our previous study.[6] Clustering analysis allows the calculation of the cluster size distribution n_S, which is the probability to find a cluster

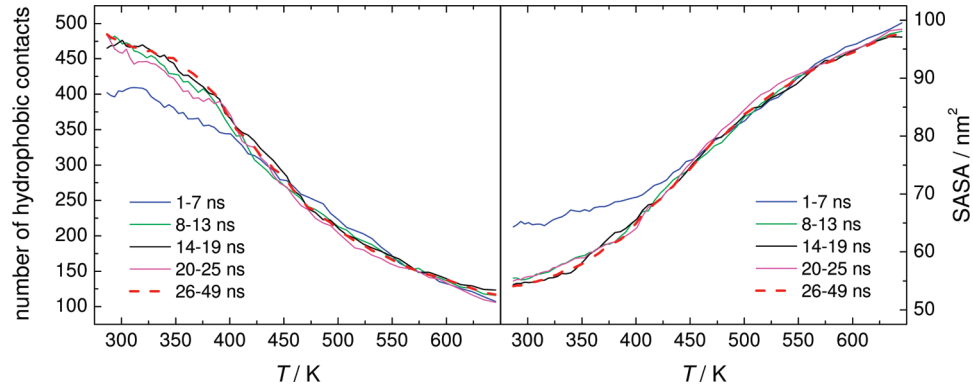

Figure 1. Average number of the hydrophobic contacts and SASA of all peptides as a function of temperature in various time intervals of the total simulation run.

containing S peptides, and distinguishing of the largest peptide cluster which consists of S_{max} peptides.

The peptide−peptide and peptide−water hydrogen bonds (H-bonds) were identified using the following criteria: an H-bond exists if the distance between the donor and the acceptor does not exceed 0.35 nm (this distance corresponds to the typical location of the first minimum in the radial distribution function between two H-bonded atoms) and if the donor-hydrogen-acceptor angle exceeds 120° (this excludes strongly distorted nonlinear H-bonds). All the oxygen atoms of the peptide were considered as hydrogen bond acceptors and all the heteroatoms having donor hydrogen were considered as hydrogen bond donors. The secondary structure was determined using the distributions of φ and ψ dihedral angles in the Ramachandran plot. A residue was considered as contributing to α-helices when $-100° \le \varphi \le -30°$ and $-90° \le \psi \le -10°$, to β-strands when $-180° \le \varphi \le -100°$ and $60° \le \psi \le 180°$, and to polyproline II structures when $-100° \le \varphi \le -30°$ and $60° \le \psi \le 180°$. Otherwise, the residue was considered as exhibiting a disordered, random-coil-like structure. The solvent-accessible surface area (SASA) of all peptides was obtained with a probe radius of 0.14 nm.

The intrinsic volumetric properties of the peptide system were studied by an approach proposed in ref 26 taking into account the difference between the volumetric properties of the hydration water and the bulk water. Water molecules were considered as belonging to the hydration shell of the peptides, if the shortest distance between their oxygen atoms and at least one of the heavy atoms of the peptides was less than 0.45 nm. This value corresponds to the average location of the first minimum in the density profile of liquid water near surfaces of various biomolecules (see refs 28 and 29, for example). The volume of the hydration layer was calculated using the following slab approximation: $V_h = \mathrm{SASA}\cdot D$, where D is the thickness of the hydration shell. As half of the typical contact distance between water oxygen and the heavy atom of a biomolecule (about 0.15 nm) is not accessible for the centers of water oxygens, D was considered to be equal to 0.3 nm.[30] The intrinsic volume V_p of the peptides was calculated as

$$V_p = L_{box}^3 - V_h - (N_0 - N_w)/\rho_b^* \qquad (2)$$

where N_w is the number of water molecules in the hydration shell of the peptides, N_0 is the total number of water molecules in the system, and L_{box} is the length of the box; ρ_b^* is the number density of bulk liquid water. The ρ_b^* values were determined from an additional series of constant-pressure simulations of pure liquid water at the same thermodynamic states as for the peptide−water system.

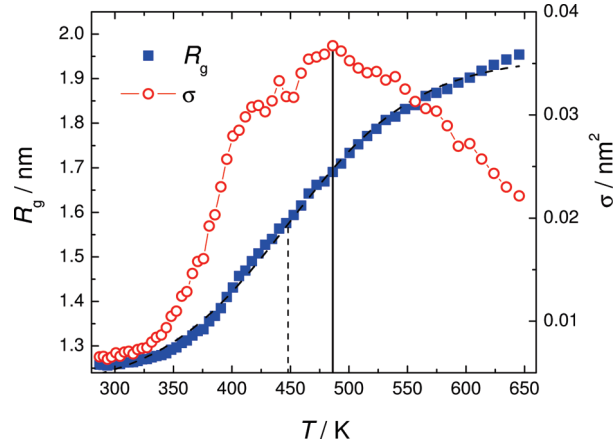

Figure 2. Temperature dependences of the radius of gyration R_g of all peptides (squares) and its mean-square fluctuations σ (circles). The temperature where σ passes through a maximum is indicated by the vertical solid line. The sigmoid fit of $R_g(T)$ and location of its inflection point are shown by dashed lines.

Results

In order to study the equilibrium thermodynamic states of the system, the initial part of the MD trajectory, where the system properties vary monotonically with time, has to be excluded. The time dependence of various system properties was analyzed by dividing the simulation run into five nonoverlapping segments and calculating the average properties of each segment. Figure 1 shows the average number of hydrophobic contacts and the SASA of all peptides for each segment of the simulation run. The number of hydrophobic contacts (Figure 1, left panel) and interpeptide H-bonds (not shown) needs the longest equilibration time of about 25 ns among all system properties studied. Other parameters, such as SASA (Figure 1, right panel) and the radius of gyration (not shown), equilibrate much faster. Based on the time evolution of all parameters studied, the equilibration period was estimated to be 25 ns and only the results obtained from the last 24 ns of the REMD simulation run are further discussed.

The radius of gyration R_g of all peptides and its mean-square fluctuations ($\sigma = \langle R_g^2 \rangle - \langle R_g \rangle^2$) were shown to be useful parameters for the characterization of the phase transition of an aqueous solution of peptides.[11,12] R_g shows a sigmoidlike increase with increasing temperature, indicating a transition from the state containing compact peptide aggregate ($R_g \sim 1.25$ nm)

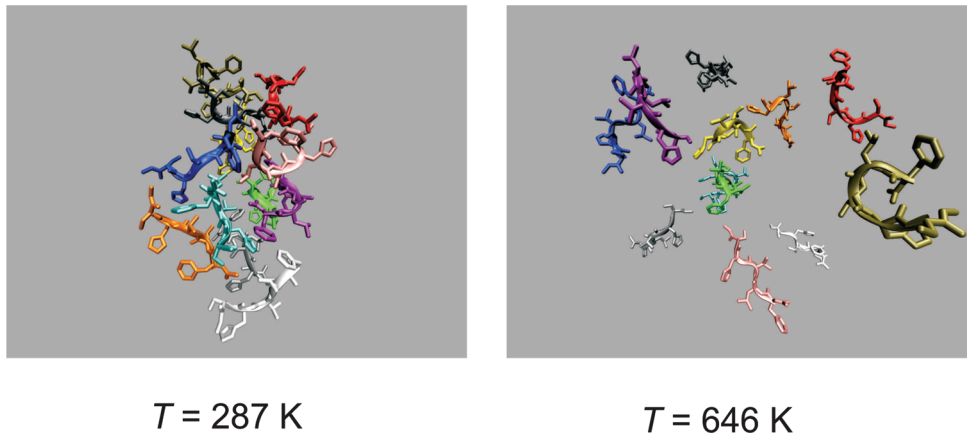

Figure 3. Examples of the arrangement of peptides in the aggregated state (left snapshot) and in the dissolved state (right snapshot).

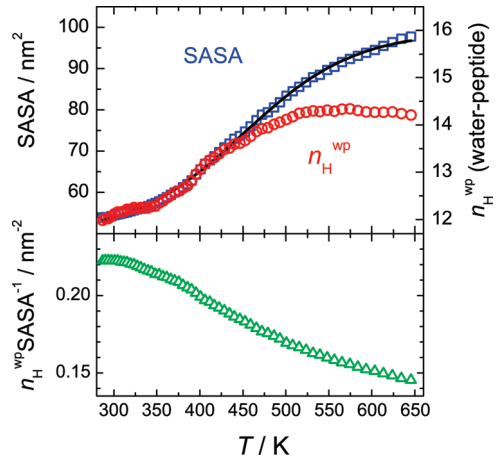

Figure 4. Temperature dependences of the SASA of all peptides (open squares), the number of peptide−water H-bonds per peptide n_H^{wp} (open circles), and their ratio (open triangles).

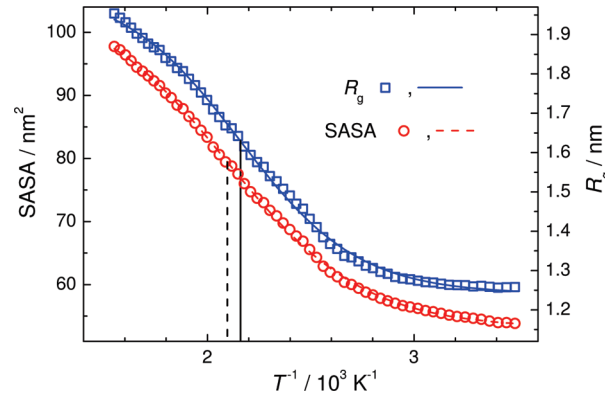

Figure 5. Radius of gyration R_g and SASA of all peptides as a function of inverse temperature $1/T$ (symbols). The fits to sigmoidal function and the locations of their inflection points are shown by solid and dashed lines.

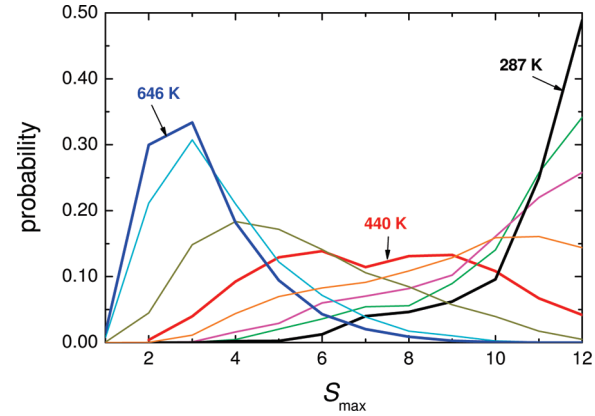

Figure 6. Probability that the largest cluster consists of S_{max} peptides calculated at T = 287, 348, 376, 401, 440, 501, 603, and 646 K.

to a disaggregated state ($R_g \sim 2$ nm) (Figure 2). Typical arrangements of peptides in these two states are shown in Figure 3 for the lowest and highest temperatures studied. The fit of the $R_g(T)$ to a sigmoid function (dashed line) indicates the midpoint of the transition at $T \approx 450$ K (vertical dashed line) and a smearing out of the transition within a range of ±55 K. A transition temperature can also be estimated using the mean-square fluctuations σ of R_g, which pass through a maximum at $T \cong 485$ K (vertical solid line). The discrepancy between the two estimations is about 35 K, which could be due to notable deviations of $R_g(T)$ from a sigmoidal shape. The temperature dependence of SASA is very similar to that of R_g and can be fitted, although not perfectly, to a sigmoidal function with the inflection point at $T \cong 450$ K (upper panel in Figure 4).

We also analyzed the behavior of the radius of gyration as a function of the inverse temperature $1/T$ (Figure 5, squares). The dependence R_g $(1/T)$ may be described by a sigmoid function almost perfectly and the goodness of the fit in this case is about two times better than that of the R_g (T) dependence. The inflection point was found to be at $T \approx 465$ K (Figure 5, solid vertical line). Similarly, the dependence of SASA on the inverse temperature $1/T$ is much closer to a sigmoid (Figure 5, circles) and the goodness of the fit is about three times better as compared to the SASA(T) dependence. The inflection point of the sigmoidal fit of SASA($1/T$) is located at $T \cong 480$ K (Figure 5, vertical dashed line).

Peptide aggregation can be quantitatively characterized utilizing clustering analysis.[6,31] The probability distributions $P(S_{max})$ to find the largest peptide cluster containing S_{max} peptides, obtained for the connectivity criterion based on the distance between the center of mass of peptides, are shown in Figure 6 for selected temperatures. At the lowest temperature studied (T = 287 K), the largest clusters consists of all 12 peptides in about 50% of the observed configurations and very rarely of less than 5 peptides. At the highest temperature studied (T = 646 K), the largest cluster usually contains 2 or 3 peptides only. At T = 440 K, the size of the largest peptide cluster strongly fluctuates, consisting of 4−10 peptides with comparable probabilities.

There is no unambiguous measure for the degree of aggregation and various properties can be used for this purpose.[6] The

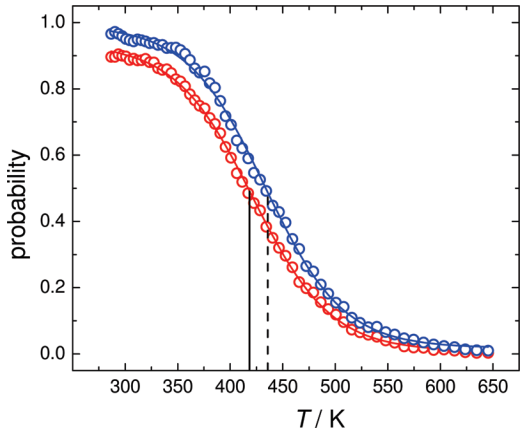

Figure 7. Temperature dependence of the probability that the largest peptide cluster includes >2/3 of all molecules (consists of more than 8 peptides). The criterion for the connectivity between two peptides was based on the distance between the centers of mass of the peptides (red circles) and on the number of hydrophobic contacts (blue circles). Fits to the sigmoidal function are shown by solid lines. The inflection points are indicated by vertical lines.

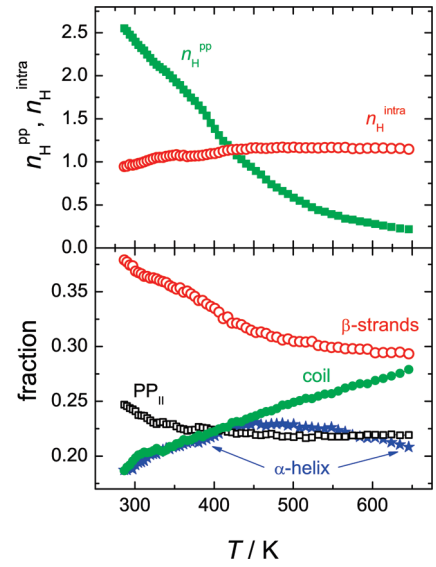

Figure 8. Number of inter- and intrapeptide H-bonds (upper panel) and populations of various elements of secondary structure (lower panel) as a function of temperature.

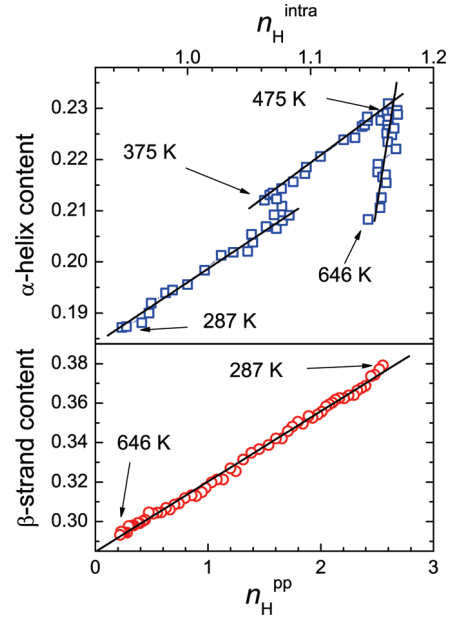

Figure 9. Correlations between α-helix and β-strand contents and the numbers of intra- and interpeptide H-bonds, respectively.

probability that the largest peptide cluster contains more than a certain percentage of the total number of peptides is one such example. For an aqueous solution of peptides, separation may be considered to occur when the aggregate includes more than 2/3 of the peptides.[6,31] Such a criterion is additionally supported by studies of phase transitions in finite lattices.[32] The temperature dependence of the degree of aggregation defined in this way is shown in Figure 7. Fits to a sigmoidal function give an inflection point at either $T = 415$ or 435 K, depending on the interpeptide connectivity criterion used.

As can be noticed from Figure 4, the average number n_H^{wp} of water−peptide hydrogen bonds per peptide and the total SASA of all peptides show quite similar change with temperature in the temperature range 287 K < T < 430 K. In particular, one additional water−peptide H-bond corresponds to an increase of SASA of about 1.1 nm^2. The temperature-induced increase of SASA above 430 K is not accompanied by the creation of new water−peptide H-bonds. This means that the peptide is not able to form H-bonds with more than about 14 water molecules. The effective hydrophilicity of the peptide surface can be characterized by the number of H-bonds with water per unit SASA. The increase of the ratio n_H^{wp}/SASA upon cooling indicates an increasing hydrophilicity of the peptide surface upon aggregation (Figure 4, lower panel). These results are in agreement with previous studies of aggregation of the same peptide at $T = 330$ K,[6] and prove that the aggregation of the peptides studied occur mainly via contacts between hydrophobic groups.

The average number n_H^{pp} of intermolecular peptide−peptide H-bonds per peptide is about 2.5 at low temperatures (Figure 8, upper panel). It continuously decreases and finally vanishes upon heating, indicating the existence of mostly peptide monomers at high temperatures. The average number of intrapeptide H-bonds n_H^{intra} increases slightly up to 450 K, thereafter remaining almost unchanged. The population of various secondary structure elements is shown as a function of temperature in the lower panel of Figure 8. In the aggregated state, which dominates at low temperatures, β-strands are the dominating structural element. The fraction of the PP_{II} conformations is about 25% at low temperatures and decreases by just a few percents upon heating. The population of disordered, random-coil-like conformations increases from 18 to 26% upon heating, whereas the α-helical content shows a nonmonotonic behavior: it increases from ∼19% at $T = 287$, passes trough a maximum (∼23%) at $T \approx 475$ K and drops down to ∼21% at the highest temperature studied.

The similarity of the temperature dependences of the β-strand content and the number n_H^{pp} of interpeptide H-bonds (Figure 8) indicates their coupling, which is expected as the β-sheets are formed due to creation of interpeptide H-bonds. The degree of such a coupling may be clearly seen when the β-strand content is shown as a function of n_H^{pp} (Figure 9, lower panel). The dependence is linear with a slope of ∼0.036 in the whole studied temperature range. As the intramolecular H-bonds are an important condition for the existence of an α-helical structure, we have analyzed the relation between these properties in the upper panel of Figure 9. Three temperature intervals with almost a linear relation between the α-helical content and n_H^{intra} can be distinguished. Up to about 450 K, both properties increase with

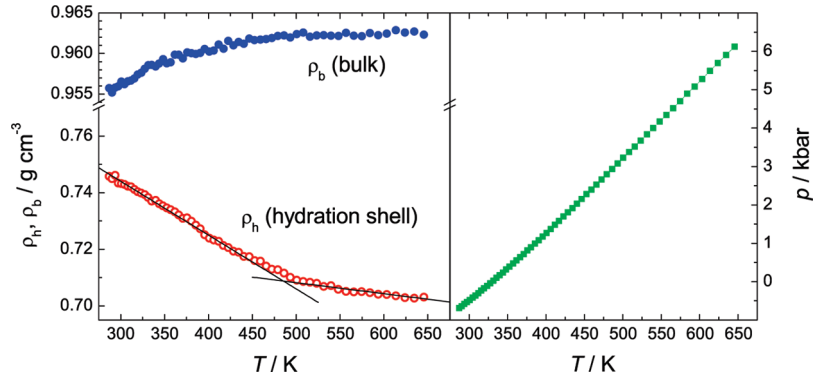

Figure 10. Temperature dependence of the water density in the bulk, ρ_b (solid circles), and in the hydration shell, ρ_h (open circles), along the simulated thermodynamic path. Corresponding pressure−temperature diagram of the constant-volume REMD simulations (right panel).

temperature due to the continuous dissolution of the peptide aggregate and some qualitative change of the correlation between the α-helical content and n_H^{intra} is seen at about 350 K. Upon heating above ∼475 K, the α-helical content starts to decrease, whereas n_H^{intra} remains almost unchanged (∼1.16). Such a behavior indicates a strong rearrangement of intrapeptide H-bonds without decreasing their total number.

Additional information about the character of peptide aggregation can be obtained from the behavior of the volumetric properties of hydration water and intrinsic volumetric properties of the peptides.[30] The density of water in the hydration shells of the peptides, $\rho_h = N_w/V_h \cdot m_w$, where m_w is the mass of a water molecule, and the density of bulk liquid water are shown in the left panel of Figure 10 as a function of temperature. ρ_h was found notably (∼25−30%) lower than the bulk density ρ_b in the same thermodynamic states, in aggreement with the strongly hydrophobic nature of the peptide's surface. The densities of both bulk and hydration water depend strongly on the thermodynamic state of a system, which is characterized by the temperature and pressure in the present constant-volume REMD simulations. The density of bulk water increases upon heating due to the strong increase of pressure with temperature (see right panel of Figure 10). In contrast, the density of hydration water decreases with temperature and the thermal expansion coefficient of the hydration water, α_h, is estimated to be 2×10^{-4} K^{-1} until $T \approx 450$ K, and 1 order of magnitude smaller at higher temperatures. The thermal expansivity of the hydration water observed in the present REMD simulations is notably smaller than that obtained for other peptides using constant temperature molecular dynamics simulations at $p = 1$ bar (0.1 MPa),[30,33] which is probably due to the high pressures at high temperatures in the constant-volume REMD simulations. However, the qualitative change in the temperature dependence of ρ_h that takes place at about 475 K cannot be attributed to the specific change of the thermodynamic state of the system, as the pressure p increases almost linearly with temperature (see right panel in Figure 10).

The intrinsic volume V_p of the peptides varies nonmonotonically along the thermodynamic path studied: it practically does not change upon heating up to $T \approx 350$ K and decreases about two times upon further heating. The temperature dependence of ln V_p is shown in the upper panel of Figure 11. The slope of the dependence ln $V_p(T)$ is equal to the intrinsic thermal expansion coefficient α_p of the peptides. The temperature dependence of ln V_p is close to linear at $375 < T < 575$ K with $\alpha_p = -2.3 \times 10^{-3}$ K^{-1} (solid line in Figure 11). The temperature dependence of the intrinsic density ρ_p of the peptides is shown in the lower panel of Figure 11. The density of the peptide

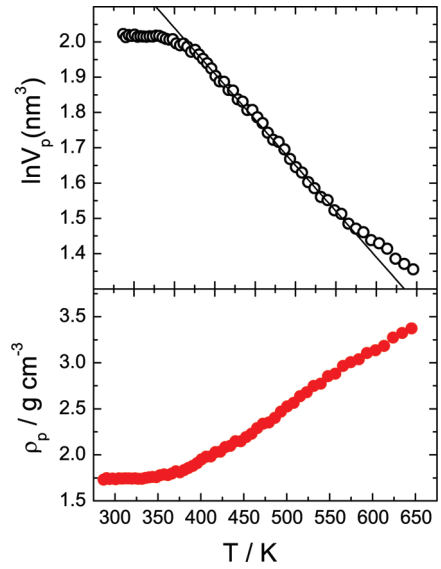

Figure 11. Temperature dependencies of ln V_p (upper panel) and the average density ρ_p of the peptides (lower panel).

aggregate is about 1.75 g/cm^3 and the density of the peptides increases upon dissolution of the aggregate, when temperature and pressure increase.

Discussion

We present the first simulation study of the effect of temperature on the aggregation of amyloidogenic peptides in explicit water. It is shown that the aqueous solution of amyloidogenic peptides, upon cooling, undergoes a transition from a one-phase state with the peptides being completely dissolved in water, to a two-phase equilibrium of a peptide aggregate with a water-rich solution. Various properties of the peptide system show a behavior similar to the conventional first-order phase transition of fluids, which is strongly smeared out in temperature due to the finite size of the simulation box. The smearing out of the transition is caused by the destabilization of the minor phase (peptide aggregate) in any finite simulated system due to thermodynamic reasons.[14] This is an intrinsic problem of any simulation study and it can be minimized by using larger systems. This problem was studied for aqueous solutions of amyloidogenic peptides, recently.[6,34] Additional rounding of the transition may originate from the exchange of configurations between the one-phase and two-phase thermodynamic states in REMD simulation methods.

We used various parameters to characterize the peptide aggregation and to locate the temperature of the demixing

transition that separates these two distinct states of the system. One kind of parameters reflects the properties of the whole system of the peptides (total radius of gyration or SASA, total number of hydrophobic contacts or H-bonds, etc). Such an approach is valid when the critical peptide concentration in the water-rich phase (solubility limit) is so small that it is effectively reproduced by pure water, whereas all the peptides in the simulation box almost permanently belong to the organic-rich phase. This situation corresponds to the aqueous solution of highly insoluble amyloidogenic peptides at low temperatures. However, upon heating, the critical peptide concentration (solubility limit) increases and reaches the average peptide concentration in the simulation box at the temperature of the phase transition. Under conditions of high critical peptide concentrations (relatively high solubility of the peptides), the essential part of the peptides belongs to the water-rich phase. In this case, the ability of the properties of the whole peptide system to describe the aggregation process largely worsens: these properties become less sensitive to the formation of peptide aggregates. As a result, the temperature dependence of these parameters is smeared out in a wide temperature range and the midpoint of the transition shifts toward higher temperatures (see dependences in Figures 1, 2, and 4). Therefore, the inflection points of these dependences (450−485 K) yield overestimated temperatures of the phase transition. By a similar analysis of the temperature-induced transition of amyloidogenic peptides in implicit water, the transition was found to be smeared out in a narrower temperature interval, despite the use of a reduced number of peptides.[11,12] This can be attributed to the lower peptide concentrations used in these studies, in comparison to the rather high weight concentration of peptides used in our study ($C = 12.4\%$).

A demixing transition can be characterized by using various clustering properties. In turn, this approach requires the establishment of a connectivity criterion between two peptides.[6] The use of a clustering analysis allows the selection of the largest peptide aggregate, which represents an organic-rich phase. This enables the characterization of the organic-rich phase, only, thereby avoiding the sensitivity of the analysis to peptide concentration. The probability distribution of the size S_{max} of the largest peptide cluster (Figure 6) evidence the largest fluctuations of S_{max} at about 440 K, which is about 45 K below the temperature, where the fluctuations of the radius of gyration of all the peptides are maximal (Figure 2).

The important characteristics of a phase transition is the order parameter, which is nonzero in the two-phase region and equal to zero in the one-phase state. In the case of a demixing transition in aqueous solutions, the order parameter corresponds to the difference of the concentrations in water-rich and organic-rich phase, respectively. Such property is ill-defined when only a few solute molecules present in the system. The probability to form an aggregate containing 2/3 of all peptides appears to be the most adequate order parameter for the temperature induced aggregation in small systems (Figure 7). This order parameter may be also used for the characterization of the degree of aggregation. A somewhat similar approach has successfully been applied for the characterization and location of the percolation transition in finite systems.[35] When using this probability and the most adequate criterion for the interpeptide connectivity based on the distance between the centers of mass of two peptides,[6] the midpoint of the transition was found to be at 415 K. This temperature should be considered as the upper limit of the demixing transition in a corresponding macroscopic system. With increasing system size, the midpoint of the transition shifts toward the transition point in the macroscopic system.[35,36] Therefore, the phase transition of the considered peptide solution in the macroscopic system can be expected to take place at about $T = 375 \pm 25$ K and $p = 0.8 \pm 0.4$ kbar. This means that the peptide aggregate could be principally destabilized by heating, but cannot be broken up at biologically relevant temperatures in a living system.

The temperature of the demixing transition obtained in the present study depends on the peptide concentration as well as on the pressure. For a fixed pressure, it should be treated as the lower bound of the liquid−liquid critical temperature in view of the arbitrarily chosen concentration of peptides. The liquid−liquid critical temperature, which is the highest temperature of the two-phase coexistence, may be observed when the concentration of peptides is equal to its critical value. (This concentration is unknown and simulations of the demixing transition at several different concentrations are necessary for its estimation.) Increasing pressure should decrease the temperature of the demixing transition, similarly to the case of molecules with low solubility in water (methane, benzene, etc.). We may expect that the temperature of the demixing transition of the considered peptide system is lower than that of a water−benzene mixture[37] and is comparable with the upper critical solution temperature of aqueous solutions of tetrahydrofuran and pyridine derivatives.[38−40]

As was shown in our previous study, at $T = 330$ K, the hydrophobic interaction is the dominating force of aggregation of the considered FLVHS peptide having methyl caps on its terminus.[6] In the present study, the same mechanism of aggregation is seen in a wide temperature range. The hydrophobic character of aggregation appears in an increasing effective hydrophilicity of the surface of the peptides exposed to water. This trend can be clearly seen from the temperature dependence of the number of water−peptide H-bonds per peptide surface area (lower panel in Figure 4). The increase of the density of hydration water upon increasing aggregation (left panel in Figure 10) also supports this conclusion. Please note, that this is not related to the effect of the decreasing temperature, as the parallel decrease of pressure reduces the density of bulk liquid water.

The intrinsic volume of the peptide aggregate does not notably depend on temperature (Figure 11), indicating a negligible thermal expansion coefficient, which is characteristic for solidlike structures. Conversely, the thermal expansivity α_p of the peptide system above the transition temperature is negative. Such behavior can be attributed to single peptides in liquid water. A negative α_p is expected for a random chain, and it was also observed for the amyloidogenic peptide Aβ_{42} and for an elastin-like peptide in water.[30] In the latter case, a random chain conformational behavior was confirmed by the analysis of the structural properties of the peptides.[41] Thus, we can attribute the negative value of α_p above the transition temperature to a random chain conformational behavior of single peptides in the disaggregated state or to the shrinkage of the inner voids of peptides with increasing temperature and pressure.

The density determined for the peptide aggregate (1.75 g/cm^3) largely exceeds the density estimated for the same peptide aggregate using its radius of gyration (0.66 g/cm^3) and assuming a spherical shape for the aggregate.[6] The origin of this discrepancy is due to the rarefied structure of the peptide aggregate, whose voids are probably partially occupied by water molecules. In the latter approach, the voids of the peptide aggregate were attributed to the volume of the aggregate, irrespective of whether they are occupied by water molecules

or not. On the other side, these two estimations of the density of the peptide aggregate allow calculation of the weight concentration of the peptides in the organic-rich phase, which was found to be ~60%. For comparison, this value is about 70% for the aqueous solution of the polymer poly(*N*-isopropylacrylamide) and about 37% for the aqueous solution of an elastin-like polymer.[42] The dissolution of the peptide aggregate upon heating causes a break up of the loosely packed structure with numerous voids, inaccessible to water molecules. The void volume in a single peptide is drastically smaller than in an aggregate which reflects the much larger value of the peptide density determined at high temperatures (Figure 11, lower panel).

β-Strands formed due to interpeptide hydrogen bonding are predominant in the secondary structure of the peptide aggregate. Interestingly, the breakup of the interpeptide H-bonds upon heating facilitates the formation of α-helical conformations (upper panel in Figure 9). Some qualitative changes in this process, presumably related to the demixing transition, occur between 350 and 375 K. However, the difference between the temperature dependence of the α-helical content and the number of intrapeptide H-bonds, occurring at about 475 K and 2.5 kbar, cannot be related to the aggregation process. The maximum of α-helical conformations at ~475 K can be attributed to a change of the conformational behavior of single peptides in liquid water. Approximately at the same state point, the temperature dependence of the density of hydration water also changes qualitatively (see left panel in Figure 10). As the density of bulk water varies gradually in this thermodynamic range, this reflects a transformation of the properties of hydration water, only. Some properties of bulk liquid water change sharply in a rather narrow pressure interval between 2 and 3 kbar,[43] which is presumably related to a weakening of the tetrahedral structure of liquid water upon pressurization.[44] This continuous transition of bulk water does not affect its density, but may affect the effective strength of water−surface interactions. The temperature dependence of the hydration water density is weaker when the water−surface interaction is stronger.[45] Hence, the crossover of $\rho_h(T)$ at $T \sim 475$ K may signal an increase of the effective water−surface interactions. However, the hydrophilicity of the peptide surface exposed to water does not undergo qualitative changes at this temperature (lower panel in Figure 4). Therefore, the crossover of $\rho_h(T)$ may be attributed to the weakening of the tetrahedral structure that makes the effective water−surface interaction stronger. We may assume that such changes in the hydration water provoke the qualitative changes observed in the conformational behavior of the peptides (Figure 9). Further studies are necessary to clarify the possible relation between the state of the hydration water and the conformational behavior of biomolecules.[46]

Acknowledgment. Financial support from the International Max-Planck Research School in Chemical Biology, the Deutsche Forschungsgemeinschaft, the European Union, and the Country North Rhine-Westfalia (Europäischer Fonds für regionale Entwicklung) is gratefully acknowledged. G.S. thanks D. Paschek for the package for REMD simulations.

References and Notes

(1) Timasheff, S. The Self-Assembly of Long Rodlike Structures. In *Protein-Protein Interactions*; Frieden, C., Nichols, L. W., Eds.; John Wiley and Sons: New York, 1981; pp 315−336.
(2) Prausnitz, J. M. *J. Chem. Thermodyn.* **2003**, *35*, 21–39.
(3) Jarrett, J. T.; Lansbury, P. T. *Cell.* **1993**, *73*, 1055–1058.
(4) Harper, J. D.; Lansbury, P. T. *Annu. Rev. Biochem.* **1997**, *66*, 385–407.
(5) Pullara, F.; Emanuele, A.; Palma-Vittorelli, M. B.; Palma, M. U. *Biophys. J.* **2007**, *93*, 3271–3278.
(6) Singh, G.; Brovchenko, I.; Oleinikova, A.; Winter, R. *Biophys. J.* **2008**, *95*, 3208–3221.
(7) Ma, B.; Nussinov, R. *Proc. Natl. Acad. Sci. U.S.A.* **2002**, *99*, 14126–14131.
(8) Zheng, J.; Ma, B.; Tsai, C.-J.; Nussinov, R. *Biophys. J.* **2006**, *91*, 824–833.
(9) Nguyen, P. H.; Li, M. S.; Stock, G.; Straub, J. E.; Thirumalai, D. *Proc. Natl. Acad. Sci. U.S.A.* **2007**, *104*, 111–116.
(10) Rohrig, U. F.; Laio, A.; Tantalo, N.; Parrinello, M.; Petronzio, R. *Biophys. J.* **2006**, *91*, 3217–3229.
(11) Cecchini, M.; Rao, F.; Seeber, M.; Caflisch, A. *J. Chem. Phys.* **2004**, *121*, 10748–1075.
(12) Baumketner, A.; Shea, J. E. *Biophys. J.* **2005**, *89*, 1493–1503.
(13) Tsai, H.-H.; Reches, M.; Tsai, C.-J.; Gunasekaran, K.; Gazit, E.; Nussinov, R. *Proc. Natl. Acad. Sci. U.S.A.* **2005**, *102*, 8174–8179.
(14) Binder, K. *Physica A* **2003**, *319*, 99–114.
(15) Mazor, Y.; Gilead, S.; Benhar, I.; Gazit, E. *J. Mol. Biol.* **2002**, *322*, 1013–1024.
(16) Swendsen, R.; Wang, J. *Phys. Rev. Lett.* **1986**, *57*, 2607–2609.
(17) Marinari, E.; Parisi, G. *Europhys. Lett.* **1992**, *19*, 451–458.
(18) Hansmann, U. H. E. *Chem. Phys. Lett.* **1997**, *281*, 140–150.
(19) Sugita, Y.; Okamoto, Y. *Chem. Phys. Lett.* **1999**, *314*, 141–151.
(20) Trebst, S.; Troyer, M.; Hansmann, U. H. E. *J. Chem. Phys.* **2006**, *124*, 174903.
(21) Periole, X.; Mark, A. E. *J. Chem. Phys.* **2007**, *126*, 014903.
(22) Simmerling, C.; Strockbine, B.; Roitberg, A. *J. Am. Chem. Soc.* **2002**, *124*, 11258–11259.
(23) Jorgensen, W. L.; Chandrasekhar, J.; Madura, J. D.; Impey, R. W.; Klein, M. L. *J. Chem. Phys.* **1983**, *79*, 926–935.
(24) Paschek, D. Volume, Temperature-Replica Exchange Molecular Dynamics with the GROMACS 3.2.1 Simulation Package. RPMDRUN−A mini-HOWTO, http://ganter.chemie.unidortmund.de/pas/ 2004.
(25) Ryckaert, J.-P.; Ciccotti, G.; Berendsen, H. J. C. *J. Comput. Phys.* **1977**, *23*, 327–341.
(26) Essmann, U.; Perera, L.; Berkowitz, M. L.; Darden, T.; Lee, H.; Pedersen, L. G. *J. Chem. Phys.* **1995**, *103*, 8577–8593.
(27) Serpell, L. C. *Biochim. Biophys. Acta* **2000**, *1502*, 16–30.
(28) Smolin, N.; Winter, R. *J. Phys. Chem. B* **2004**, *108*, 15928–15937.
(29) Brovchenko, I.; Krukau, A.; Smolin, N.; Oleinikova, A.; Geiger, A.; Winter, R. *J. Chem. Phys.* **2005**, *123*, 224905.
(30) Brovchenko, I.; Burri, R. R.; Krukau, A.; Oleinikova, A.; Winter, R. *J. Chem. Phys.* **2008**, *129*, 195101.
(31) Singh, G.; Brovchenko, I.; Oleinikova, A.; Winter, R. Aggregation of fragments of the Islet Amyloid Polypeptide as a phase transition: A cluster analysis. *Proceedings of the NIC Workshop "From Computational Biophysics to Systems Biology"*, NIC Series; 2007, pp 275−278.
(32) Nussbaumer, A.; Bittner, E.; Neuhaus, T.; Janke, W. *Europhys. Lett.* **2006**, *75*, 716–722.
(33) Mitra, L.; Oleinikova, A.; Winter, R. *ChemPhysChem* **2008**, *9*, 2779–2784.
(34) Pawar, A.; Favrin, G. *PLoS ONE* **2008**, *3*, e2641.
(35) Oleinikova, A.; Brovchenko, I. *Mol. Phys.* **2006**, *104*, 3841–3855.
(36) Partay, L. B.; Jedlovszky, P.; Brovchenko, I.; Oleinikova, A. *Phys. Chem. Chem. Phys.* **2007**, *9*, 1341–1346.
(37) Rebert, C.; Kay, W. *AIChE J.* **1959**, *5*, 285–289.
(38) Brovchenko, I.; Oleinikova, A. *J. Chem. Phys.* **1997**, *106*, 7756–7765.
(39) Narayanan, T.; Kumar, A. *Phys. Rep.* **1994**, *249*, 135–218.
(40) Balevicius, V.; Weiden, N.; Weiss, A. *Ber. Bunsenges. Phys. Chem.* **1994**, *98*, 785–792.
(41) Krukau, A.; Brovchenko, I.; Geiger, A. *Biomacromolecules* **2007**, *8*, 2196–2202.
(42) Urry, D.; Hugel, T.; Seitz, M.; Gaub, H.; Sheiba, L.; Dea, J.; Xu, J.; Parker, T. *Philos. Trans. R. Soc. London B* **2002**, *357*, 169–184.
(43) Krisch, M.; Loubeyre, P.; Ruocco, G.; Sette, F.; D'Astuto, M.; Toulec, R. L.; Lorenzen, M.; Mermet, A.; Monaco, G.; Verbeni, R. *Phys. Rev. Lett.* **2002**, *89*, 125502.
(44) Oleinikova, A.; Brovchenko, I. *J. Phys.: Condens. Matt.* **2006**, *18*, S2247−S2259.
(45) Oleinikova, A.; Brovchenko, I.; Winter, R. *J. Phys. Chem.* **2009**, *113*, 11110–11118.
(46) Oleinikova, A.; Brovchenko, I. *ChemPhysChem* **2008**, *9*, 2659–2702.

JP901144V